Acoustical characterization of different micro-perforated absorbers in confined spaces under moderate Mach number flow condition

Sebastian Floss[1], Andreas Mutschlechner[1] and Manfred Kaltenbacher[1,2]
[1] *Institute of Mechanics and Mechatronics, TU Wien, Vienna, Austria*
[2] *Institute of Fundamentals and Theory in Electrical Engineering, TU Graz, Austria*

Introduction

Using micro-perforated absorbers (MPA) [3] in an environment with a non-stationary background medium has been shown to be effective in reducing noise [1]. Static pressure losses were not significantly increased, which led to the conclusion that at least in a straight flow scenario, the commercially available slit shaped micro-perforated plates (Acustimet^{TM}) guide the flowing air. However, an interaction effect of flow and acoustic field (static pressure losses altered and non beneficiary changes in the emitted sound spectra) were visible when the micro-perforations were perfused. These effects might further change with porosity, slit size, flow direction and nature of the back volume cavity (locally and non-locally reacting liner).

In this contribution, we investigate the effect of different flow states and material parameters on the sound absorbing performance of various MPA structures. The test rig is based on the two-port theory using the transfer matrix method with two sources [2].

Since the microphones are used in a turbulent flow environment, wall-pressure fluctuation associated with vortical flow structures, will manifest as additional pseudo-sound [4] at the microphone membranes. To minimize this impingement and its effect on the transmission loss (TL) characterization measurements, special denoising measures were applied.

Test rig

The measurements were conducted in an elongated duct with quadratic cross section ($h = 25$ mm). Two pairs of 1/4" condenser microphones, measuring pressure fluctuations, were placed in duct section 1 and 2 (indicating source locations) separated by $s = 20$ mm. This allows measurements across a range of roughly 6400 Hz with a Mach number of $Ma = 0.1$ ($f_{\text{cut-off}} = c_0/2h \cdot (1 - Ma^2)$, with c_0 as speed of sound).

Figure 1a shows the schematic of the rig with microphone positions, source location and flow direction. The expected flow velocity profile and a magnification of the microphone section with cavity (orange tagged) and protective wire mesh (red) is displayed in Figure 1b. Both measures were applied to reduce pseudo-sound spectra. A sinus sweep signal was used to achieve a higher signal-to-noise ratio of the deterministic signal compared to the turbulent flow induced pseudo-sound.

Measurements were done when a stationary flow state was reached , which was determined when pressure sensors up and downstream of the test object showed a stable static pressure loss. The flow state ($\nu = 15.72 \times 10^{-6}$ ($\mathrm{T} = 24°C$), $v_{\text{mean}} = v_{\text{m}} \approx 20\ \mathrm{m\,s^{-1}}$, $h = 25$ mm) can be characterized as fully turbulent, with $Re = vh/\nu \approx 31000$. The largest reachable Ma number, before turbulent pressure fluctuations became dominant was $Ma \approx 0.1$.

The acoustic transmission loss computes by [2]

$$\begin{bmatrix} T_{11} & T_{12} \\ T_{21} & T_{22} \end{bmatrix} = \begin{bmatrix} p_{\text{a}}^1 & p_{\text{a}}^2 \\ u_{\text{a}}^1 & u_{\text{a}}^2 \end{bmatrix}_{x=0}^{-1} \begin{bmatrix} p_{\text{a}}^1 & p_{\text{a}}^2 \\ u_{\text{a}}^1 & u_{\text{a}}^2 \end{bmatrix}_{x=l} \quad \text{and} \tag{1}$$

$$TL = 10 \log \left(1/4 \left| T_{11} + T_{12}/Z_0 + T_{21} Z_0 + T_{22} \right|^2 \right), \tag{2}$$

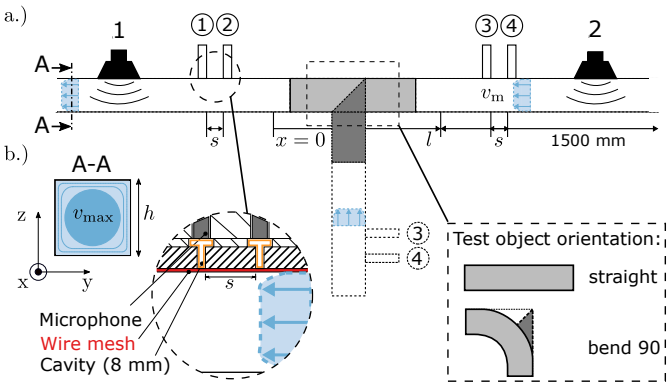

Figure 1: a.) Test rig scheme with source locations (1,2) and microphone positions (1-4); b.) qualitative velocity profile in quadratic cross section, magnification of microphone locations and orientation of test objects

with acoustic pressure p_{a} as measurable quantity and acoustic particle velocity u_{a} as from pressure derived quantity. Index 2 refers to data acquired with source upstream and 1 refers to data acquired when the source was downstream. The overall length of the test section was $l = 280$ mm (includes pressure measurement sections up and downstream next to the test object). The test object length was 200 mm.

Materials

The test objects under consideration had different orientation (see Figure 1, straight and a 90 °-bend), different back volume shapes and length. Most importantly, however, the micro-perforated material, building the absorber structure, differed in slit size and perforation rate. Since this is a pre-study, the exact values of those parameters were not determined.

Figure 2 shows that material A and B differ slightly in slit size, but are rather equal in perforation ratio. Most

significantly, material A was milled after the perforation procedure. Material H is a wire mesh and has a rather high perforation rate and small slit size compared to A and B. Material X has roughly one third of the slit size of B with a corresponding smaller perforation rate. Material Y has the smallest slit size and perforation rate of all tested materials.

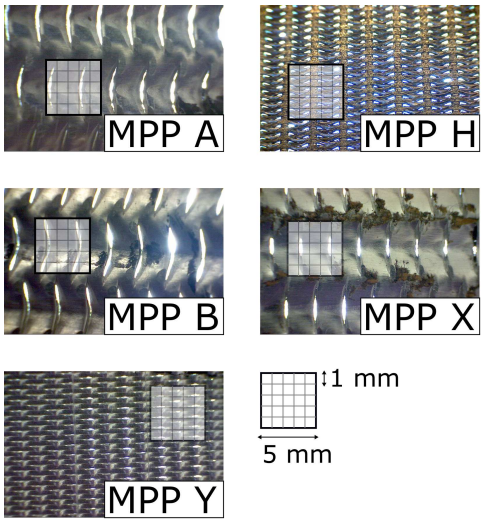

Figure 2: Investigated micro-perforated materials with different slit sizes and perforation rates; comparison with the indicated square of length 5 mm

TL results of MPA structures

The following figures show the characterizing transmission loss for every test object with different flow speeds and directions. The results also help to determine the applicability of the four microphone transfer matrix method with a background mean flow for more complex absorber structures. This concerns pseudo sound and convection damping effects.

One has to keep in mind [5] that the pseudo-sound measured by a microphone is assumed to be caused by turbulent pressure fluctuations in the airflow interacting with the microphone diaphragm. The frequency f_{turb} of the pressure fluctuation caused by the convection of a turbulent eddy of correlation length l_{turb} convecting with velocity order $\sim v_{\mathrm{m}}$ past the microphone diaphragm should be approximately equal to $v_{\mathrm{m}}/l_{\mathrm{turb}}$. The frequency of a microphone's pseudo noise spectrum scales as

$$\frac{f_{\mathrm{turb}}\delta}{v_{\mathrm{m}}} \tag{3}$$

where f_{turb} is the one third-octave band centre frequency and δ is a length scale set equal to the 1/4" microphone diaphragm diameter ($\delta = 6.35$ mm). For frequencies where $f_{\mathrm{turb}}\delta/v_{\mathrm{m}} \sim 1$ (as a measure of aerodynamic compactness) the correlation lengths of the pressure fluctuations on the diaphragm surface are of the same size as microphone diaphragm diameter and will tend to cancel each other out. This "spatial averaging" effect is in this case beneficial and will result in a drop-off of the measured pseudo-sound level.

To help with the interpretation reference lines are shown. The red dashed line represents a 3 dB constant transmission loss and the black dashed a frequency of ≈ 4800 Hz. In this region the pressure data matrix at $x = 0$ in (1) is ill-conditioned, because of a pressure dip in the standing wave pattern at microphones positions. When different flow states are compared the dark red line always indicates the no flow case.

The reference measurements are depicted in Figure 3 and represent the case for a straight flow scenario and quadratic cross section with no back volume cavity.

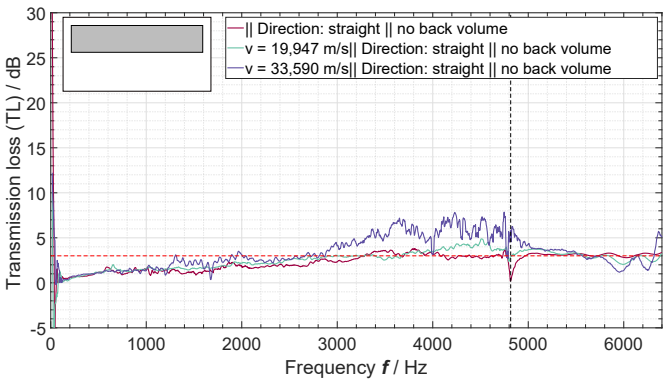

Figure 3: Reference straight test section measurements; red dashed line represents 3 dB transmission loss; black dashed line representing a pole in frequency response function of the test rig

First, one notices a rather constant increase of transmission loss per frequency for the now flow case. This behaviour is attributed to the acoustic damping effect of the protection grid covering the microphone pinhole.

One can see that the no flow case and 20 m/s are rather similar, but at ~ 30 m/s the transmission loss due to flow effects is increasing. Several physical phenomena might play together here. First, the frequency range 4000 to 5000 Hz might be affected from the afore-mentioned ill-conditioned pressure data and thus an error prone calculation of TL in (2). Furthermore, the cavity and pinhole beneath the microphones (orange tagged in Figure 1 b) might act as a Helmholtz resonator with its own frequency response function. This could be responsible for the transmission loss increase when flow velocity increases.

Also convection might increase acoustic damping since the speed of sound c_0 is modulated with $(1 \pm Ma)$ downstream (+) and upstream (-). Also, the modification of particle velocity of the sound waves due to the turbulent flow field (compare Figure 1 b) is inhomogeneous in the y-z-plane. On could argue that when the sound waves propagate through the mean flow boundary layer, the mean shear flow would refract the downstream waves towards the wall, and the upstream waves towards the center. This would result in more damping of the downstream wave, since more acoustic energy are guided to the acoustic boundary layer where the visco-thermal losses are significant; for the upstream wave, the outcome is supposed to be opposite [6]. Above 5000 Hz the smoother spectrum might be partially caused by the spatial averaging described before.

The first comparison of material A,B and H is shown in Figure 4. One can see that material H with higher perforation rate results in a significantly higher transmission loss. Below a frequency of 1000 Hz there is almost no difference visible. This confirms previous studies showing that in a quiescent medium only geometrical changes of the cavity can influence the TL in that region significantly. Also there is a 2 to 3 dB difference in absolute resonance peaks in the vicinity of 3000, 4000 and 6000 Hz between material A and B. Again, material A was milled which might have led to a changed slit size or shape. Notably, this is only visible at cavity resonances.

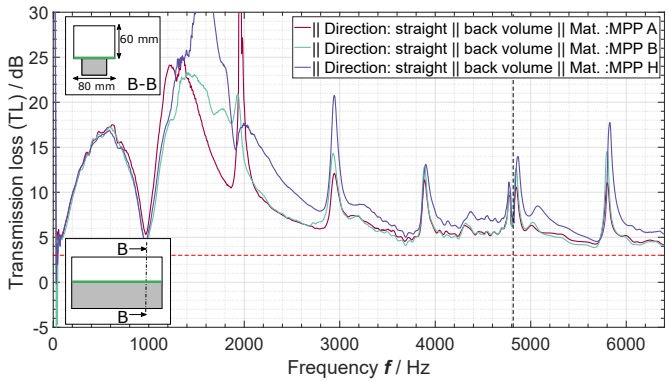

Figure 4: Straight test section with 60x80 mm back volume cavity; in B-B schematic the green line represents the location of the micro-perforated material

Due to its rather large perforation rate and thus presumably allowing an easier perfusion, material H was chosen for the flow state comparison. Figure 5 shows that the flow grazing the micro-perforation (supposable interaction of velocity shear layer and acoustic particle velocity, especially at resonances) has an TL increasing effect below 1000 Hz. This even more pronounced in the region of 2000 to 3500 Hz at resonances. Interestingly, the opposite effect is visible in the region of 6000 Hz.
The dimension of the back volume cavity allows the propagation of higher order modes (non-local reaction) at roughly 2000 Hz. In this region up to 3500 Hz the TL increasing effect of velocity occurs in more broadband fashion. It has to be determined if these two physical effects are correlated.

Following the parameter study outline, the next step is to change the flow direction. The bend reference measurement with 3 dB (red dashed)) and frequency singularity reference from the straight flow case can be seen in Figure 6. The transmission loss below $\sim$ 30 m/s is similar to the straight flow case with an increase of roughly 2 dB below 1000 Hz which might be connected to the geometrical change. The higher frequency regime seems unaffected. Now at $\sim$ 30 m/s one can see a larger spurious TL trend. An explanation could be a larger influence of the shear flow-acoustic field interaction, since additional velocity gradients are introduced due to the bending. One can see two pronounced increased TL regimes between 1000 to 2000 Hz and 3000 to 4000 Hz.

The influence of the bended back volume with different

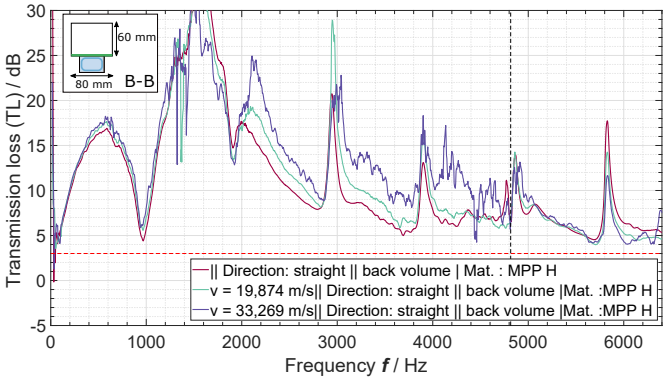

Figure 5: Straight test section with 60x80 mm back volume cavity and different flow speeds; in B-B schematic the green line represents the location of the micro-perforated material

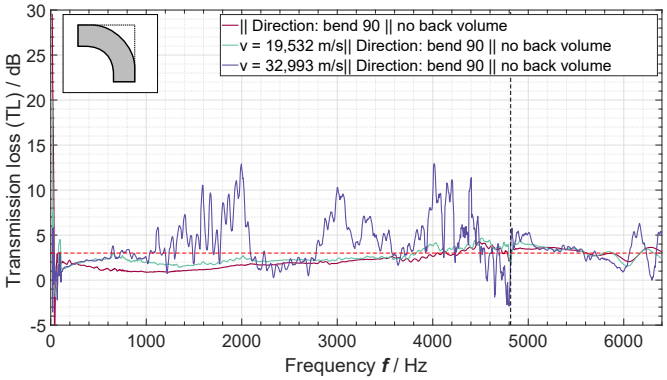

Figure 6: Bend straight 90 turn and different flow speeds

micro-perforated materials can be seen in Figure 7. Due to the bending the material parameter slit size might have changed a little for material A and B, but the overall trend in comparison is the same. At roughly 1300 Hz a presumed plate mode decreases the TL strongly. Material H is more flexible and thus shows a less pronounced decrease due to a smaller resonance response. The plate modes is also visible in Figure 5; in both cases the micro-perforated plates had the same length.

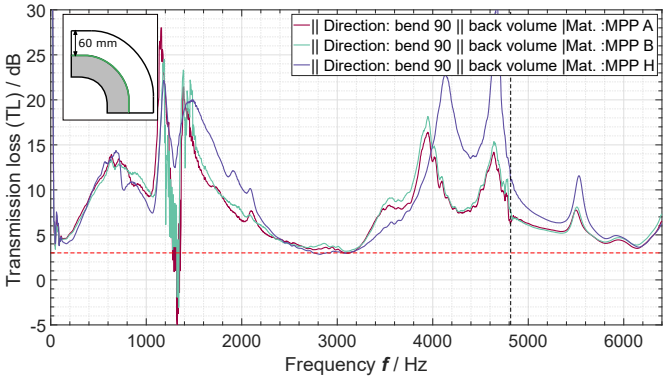

Figure 7: Bend straight 90° turn and different materials in bended form (green in schematic B-B)

The bended case with flow in Figure 8 shows that the transmission loss is now increased between 900 to roughly

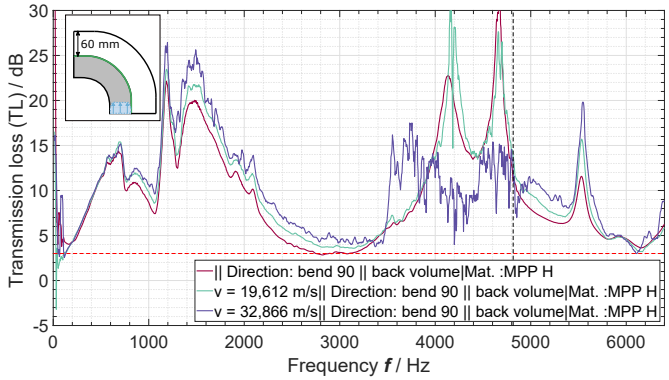

Figure 8: Bend straight 90° turn and different flow speeds

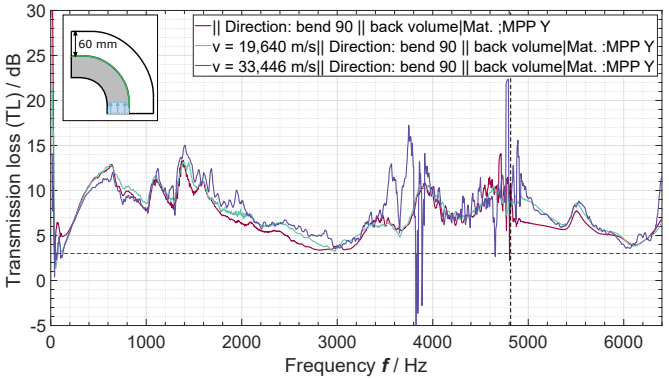

Figure 10: Material Y bended at different flow speeds

3200 Hz with an almost constant offset. Now in contrast to the straight flow case (see Figure 5) we can see an increase in transmission loss (at 5500 Hz) in the higher frequency regime. In the region below 800 Hz, the differences in TL between the two flow and no flow states are almost indiscernible. Comparing with Figure 6, one see that this is not the case here. The signal to noise ratio was sufficient since the trend in TL is qualitatively similar to the no flow case. Up to 3000 Hz the spurious pseudo-sound related transmission loss is superposed by the transmission loss calculated from the deterministic signal measurements.

The TL plots for materials X and Y are displayed in Figures 9 and 10 and show that a decrease in perforation rate and slit size also decreases the transmission loss. However, the transmission loss is more broadband and cavity resonance peaks are not as pronounced as in the preceding cases. Since the back volume is the same and $\lambda/4$ particle velocity peaks should appear as before, a conclusion could be that the acoustic and flow induced perfusion is hindered by the smaller slit size and perforation rate. This effect seems to be higher for material Y compared to material X when examining the flow state transmission loss up to 3000 Hz. However, one has to keep in mind that spurious TL trends are high in this frequency region. After the singularity region at $\approx$ 4800 Hz, we see a similar trend as in Figure 8, the transmission loss increases with increasing flow velocity.

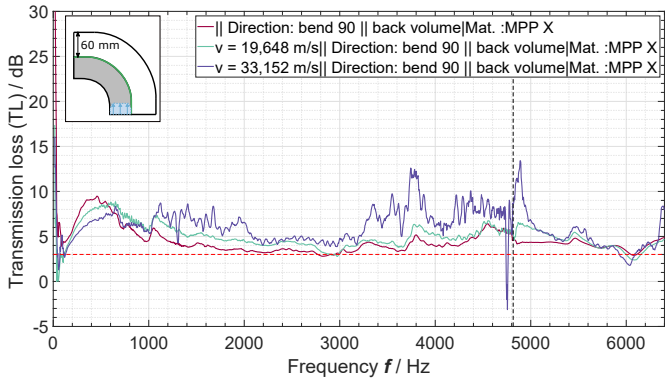

Figure 9: Material X bended at different flow speeds

Conclusion

We have shown the effects of flow velocity and flow direction on the acoustic absorption properties of various micro-perforated absorbers with and without back volume cavity. Plate materials with differences in slit size and perforation rate have been examined. It could be shown that the 2 pole network measuring techniques works for more complex test objects (orientation and flow direction). Denoising measures like microphones recessing and covering and a large signal to noise ratio, help to discern acoustics from pseudo-sound induced by turbulent flow structures impinging on the microphone diaphragma.

A general conclusion is that the effectiveness of the MPA in non-quiescent medium changes with flow direction, speed and material parameters. Further free field measurements have been conducted and will be used to determine flow influence correction parameters for the Johnson-Champoux-Allard-Lafarge (JCAL) model. The presented transmission loss data will be used as validation benchmark.

References

[1] Floss, S., Czwielong F., Krömer F., Becker, S. and Kaltenbacher, M.: Achieving axial fan sound reduction with micro-perforated absorbers, Fortschritte der Akustik - DAGA 2019, Rostock, 2019

[2] Abom, M.: Measurement of the scattering-matrix of acoustical two-ports, Mechanical Systems and Signal Processing 1991 (5)2, 89-104

[3] Maa, D.-Y.: Potential of the microperforated panel absorber, J. Acoust. Soc. Am. 1998 104 (5)

[4] Roger, M.: Microphone measurements in aeroacoustic installations, STO, STO-EN-AVT-287

[5] Pearse, J.: Measurement of sound in air flow, ICSV-13 Vienna

[6] Weng, C.: Theoretical and numerical studies of sound propagation in low-Mach-number duct flows , 2015, PhD-Thesis, KTH